phys. stat. sol. (b) **245**, No. 3, 511–520 (2008) / **DOI** 10.1002/pssb.200777704

physica status solidi b
www.pss-b.com
basic solid state physics

On the properties of auxetic meta-tetrachiral structures

Joseph N. Grima*, Ruben Gatt, and Pierre-Sandre Farrugia

Department of Chemistry, Faculty of Science, University of Malta, Msida MSD 2080, Malta

Received 3 July 2007, revised 14 November 2007, accepted 9 December 2007
Published online 12 February 2008

PACS 62.20.–x, 81.05.Zx

* Corresponding author: e-mail joseph.grima@um.edu.mt, www.auxetic.info

Auxetics are systems which get fatter when stretched and thinner when compressed i.e. they exhibit a negative Poisson's ratio. Here, we present an analysis of a novel class of structures (referred to as 'meta-chiral') which belong to the class of auxetics constructed using chiral building blocks. We show through analytical modelling that some of these systems can exhibit negative Poisson's ratios, the extent of which will depend, amongst other things, on the geometry of the system.

1 Introduction Auxetic materials [1], also known as 'anti-rubber' [2] or 'self-expanding' [3], behave in a counterintuitive way, in that they experience a lateral expansion when they are uniaxially stretched and a lateral contraction when compressed. This is in contrast with most everyday, or conventional materials which do the opposite, i.e. they expand when stretched and contract when compressed.

The extent of expansion/contraction that accompanies a uniaxial strain in the orthogonal direction is measured through the Poisson's ratio. More specifically, the Poisson's ratio ν_{ij} in the $Ox_i - Ox_j$ plane for loading in the Ox_i direction is defined as the negative ratio of the transverse strain ε_j over the applied strain ε_i. In conventional materials, the sign of the Poisson's ratio is positive since a positive ε_i is accompanied by a negative ε_j and vice-versa and in fact, most everyday materials such as plastics and metals have a positive Poisson's ratio, for example, the Poisson's ratio of most single crystals and metals ranges from 0.20 to 0.27, while the Poisson's ratio of soft metals ranges from 0.30 to 0.40 [4]. However, in auxetic materials, both strains have the same sign and thus the Poisson's ratio assumes a negative value. Such a negative value is permitted in the theory of elasticity, where it may be shown that the Poisson's ratio can range from $-1 \le \nu \le +0.5$ for isotropic three-dimensional materials [5], within the range $-1 \le \nu \le +1$ for two-dimensional isotropic systems [6], whilst there are no limits on the Poisson's ratios of anisotropic systems.

In recent years, a number of auxetic materials and structures have been extensively described in Refs. [6–38]. In all of these systems the negative Poisson's ratio is a result of the particular geometrical setup and the deformation mechanism this geometry undergoes when subjected to a stress. It is also important to note that auxetic behaviour is a scale independent property and therefore the same mechanism can operate at the macro, micro and nano level.

Auxetics have many applications, not only because they get wider when stretched but also because of the many beneficial effects in the other materials' properties which come as a result of having a negative Poisson's ratio. These include a higher resistance to indentation [39, 40], improved acoustic properties [41] and a natural tendency to form dome-shaped surfaces [1] – something which conventional materials never do.

A configuration that has attracted considerable attention in recent years in view of its potential for exhibiting negative Poisson's ratios is the hexagonal chiral system, proposed as a concept by Wojciechowski [13] and later implemented as a two-dimensional periodic structure by Lakes [42]. Lakes' hexagonal chiral honeycomb (see Fig. 1a) may be considered as being constructed from units (building blocks, highlighted in bold in Fig. 1a), which may be described as a central cylinder (henceforth referred to as 'node') with six tangentially attached ligaments, where the ligaments are arranged in such a way that this basic unit exhibits rotational symmetry of order six. This type of connectivity makes the basic unit 'chiral' (i.e. it may be constructed as 'left handed' or 'right handed', where the two versions are not super-imposable but are

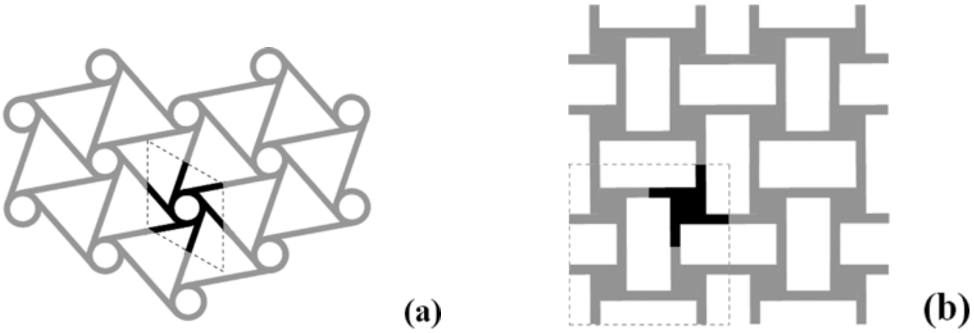

Figure 1 (a) The 'chiral honeycombs' proposed by Lakes (1991) and (b) the 'anti-tetrachiral' network proposed by Sigmund and co-workers (1998). Note that the 'basic chiral units' are highlighted in bold whilst the size of the tessellatable unit cell is highlighted by the dotted lines.

mirror images of each other) and the honeycomb so constructed is made up only of basic units with the same chirality and is also chiral.

Another auxetic system with similar characteristics was suggested by Sigmund and co-workers [43] (see Fig. 1b), who proposed a three dimensional structure, which in one projection exhibits some similar features to the system described by Lakes. Like Lakes's hexagonal honeycomb, Sigmund's system in Fig. 1b has a basic unit (highlighted in bold in Fig. 1b) that may be described as a central node with four tangentially attached ligaments which are arranged in such a way that the basic unit exhibits its rotational symmetry, this time of order four. However, although this basic unit is chiral, Sigmund's honeycomb contains equal amounts of 'left handed' and 'right handed' basic units and is not chiral (it is racemic).

If Lakes' and Sigmund's structures in Fig. 1 are constructed in such a way that the thin ligaments are welded to the nodes, then a uniaxial on-axis load will result in a rotation of the nodes accompanied by flexure of the ligaments. This type of deformation results in 'folding' of the ligaments around the node when the honeycombs are subjected to compressive loading and 'unfolding' when they are subjected to tensile loading, a behaviour that results in auxeticity. In fact, Prall and Lakes [9] performed a theoretical and experimental investigation of their hexagonal system and concluded that it exhibits a Poisson's ratio of –1 for in-plane deformations. They also showed that, in contrast with most other negative Poisson's ratio materials, the Poisson's ratio of their system is maintained over a significant range of strain.

Lakes's and Sigmund's structures are in fact only two examples of a larger set of two dimensional structures that can be constructed from chiral building blocks exhibiting rotational symmetry of order n [38]. In two-dimensions[1], such basic units may be connected together either with the nodes on the same side of the ligaments (as in the case of Sigmund's system) or with the nodes on opposite sides of the ligaments (as the case of Lakes's system), and, although there are an infinite amount of such chiral building blocks exhibiting rotational symmetry of order n, where n is the number of ligaments attached to each node, only the building blocks where n = 3, 4, or 6 may be used to construct space filling periodic structures [38]. In fact, unless the symmetry constraints are relaxed, only five such periodic structures can exist as illustrated in Fig. 2 where in the case where the two nodes are on opposite sides of the ligaments, all the repeat units in the structure have the same chirality and the resulting structure is also chiral (as Lakes's honeycomb with n = 6) whilst when the nodes are on the same side of the ligaments, the structures will require an equal amount of basic units of both chiralities, and the resulting structures are non-chiral ('racemic', as was Sigmund's honeycomb with n = 4). A systematic nomen-

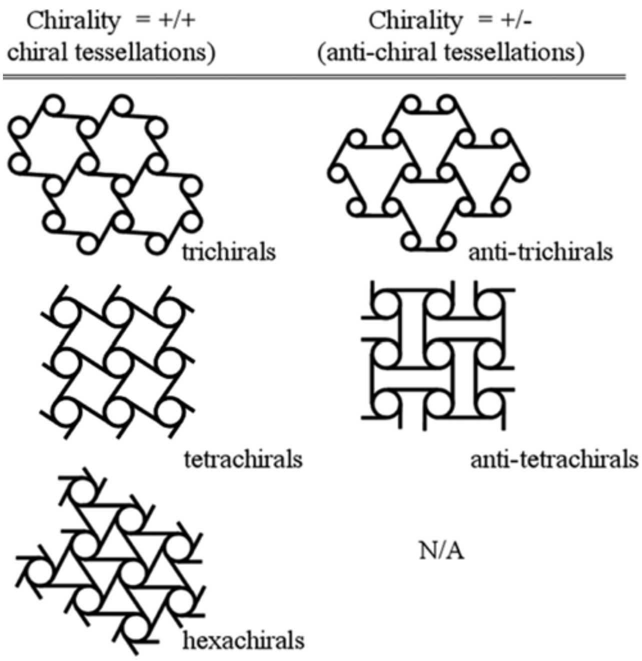

Figure 2 Five tessellations that may be obtained from the 'chiral' basic units exhibiting rotational symmetry of order n. Note that more systems can be obtained if the constraint that the basic units exhibits rotational symmetry of order n is relaxed.

[1] We note that this concept of 'unfolding of chiral unit' may also be extended to three-dimensional building blocks, a process which would lead to various other auxetic structures.

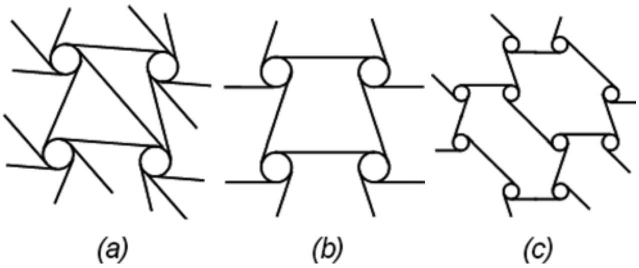

Figure 3 Examples of meta-chirals systems for systems having (a) six (b) four and (c) three ribs attached to each node. Note that for all systems, the ligaments are always attached tangentially to the nodes in such a way that they protrude out from the circles in the same direction to form 'chiral' sub-units but the ligaments are not attached to the rods in a rotationally symmetric manner where the order is equal to the number of rods. Also note that within the same structure there are some nodes which are attached to the same side of the ligaments (as in the chirals) and some others attached to opposite sides of the ligaments (as in the anti-chirals), hence the name 'meta-chirals'.

clature for these systems is described in Fig. 2, where the chiral systems with the nodes on opposite sides of the ligaments are termed as hexachiral, tetrachiral and trichiral (for $n = 6$, 4 and 3 respectively) whilst the 'racemic' systems with the nodes on the same sides of the ligaments are referred to as anti-tetrachiral and anti-trichiral (for $n = 4$ and 3 respectively).

In this paper, we show that by relaxing the constraint that the basic chiral unit exhibits rotational symmetry of order n, where n is the number of ligaments attached to each node, it becomes possible to construct various other such systems including systems which we shall henceforth refer to as meta-chirals (see Fig. 3). These systems share some basic properties of the chirals and anti-chirals in the sense that they are made up of chiral building blocks made from circular nodes connected together through ligaments. However, their rotational symmetry is not equal to the number of ligaments attached to each node, and also, within the same structure there are some nodes which are attached to the same side of the ligaments (as in the chirals) and some others attached to opposite sides of the ligaments (as in the anti-chirals), hence the name 'meta-chirals'. We analyse one such metachiral system, in particular the meta-tetrachiral system illustrated in Fig. 4 for which we derive and discuss in detail expressions for the on-axes Poisson's ratios of such systems which deform through hinging at the joints between the ligaments and the nodes, thus showing that these systems also exhibit some very interesting properties, including auxetic behaviour.

2 Modelling of systems where rigid ligaments are connected to rectangular-shaped rigid nodes through flexible hinges: idealised hinging model

The geometry of the structure considered for the 'idealised hinging model' has the nodes in the form of rectangles of dimensions $a \times b$ which are connected together through ligaments of lengths A and B as illustrated in Fig. 4. To distinguish between the two nodes present within a single unit cell, we have labelled them '1' and '2' as shown in Fig. 4.

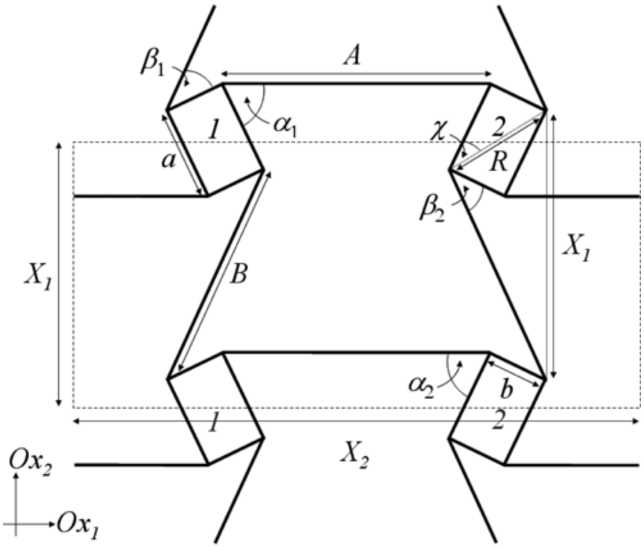

Figure 4 Geometry of the metachiral system made from rectangular nodes.

Likewise, we have denoted the angles between the ligaments of length A and nodes '1' and '2' as α_1 and α_2 respectively, whilst the angles between the ligaments of length B and nodes '1' and '2' as β_1 and β_2 respectively. We note that if α_1, α_2, β_1 and β_2 are such that in the undeformed state, the unit cell is rectangular (see below), through symmetry, uniaxial on-axis loading will not result in any shear strain with the result that the change in the angle α_1 is equal to the change in α_2 whilst the change in the angle β_1 is equal to the change in β_2. Thus, in this derivation we will assume that $\alpha_1 = \alpha_2 = \alpha$ and $\beta_1 = \beta_2 = \beta$. (Note that these relationships may not hold if the system is subjected to a shear strain.)

For this system, the projections of the unit cell in the Ox_i directions ($i = 1, 2$) may be given by

$$X_1 = 2[A + b\sin(\alpha) - a\cos(\alpha)] = 2[A - R\cos(\alpha + \chi_R)] \,, \tag{1}$$

$$X_2 = \sqrt{R^2 + B^2 - 2RB\cos\left(\frac{\pi}{2} - \chi_R + \beta\right)} = \sqrt{R^2 + B^2 + 2RB\sin(\beta - \chi_R)} \,, \tag{2}$$

where

$$R = \sqrt{a^2 + b^2} \quad \text{and} \quad \chi_R = \tan^{-1}\left(\frac{b}{a}\right). \tag{3}$$

Also, we note that for rectangular unit cells, the angle α is related to the angle β, i.e. the two angles are not independent of each other. The relationship between these two angles can be derived by referring to Fig. 5, where we note

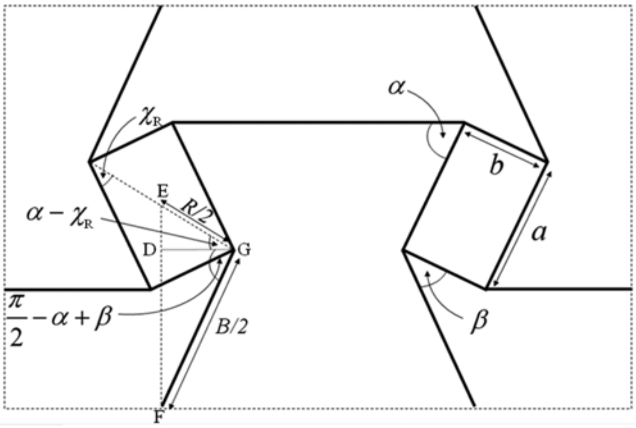

Figure 5 Parameters used for the relation between α and β.

that for triangle DEG, the length DG, where DG is perpendicular to EF is given by

$$|\mathrm{DG}| = \frac{R}{2}\cos(\alpha - \chi_R) = \frac{B}{2}\cos\left(\frac{\pi}{2} - \alpha + \beta\right) \tag{4}$$

and thus

$$\alpha = \chi_R + \tan^{-1}\left[\frac{R - B\sin(\beta - \chi_R)}{B\cos(\beta - \chi_R)}\right]. \tag{5}$$

In this way, for uniaxial loading, the unit cell parameters X_i are functions of the single variable β, i.e. using the chain rule, the Poisson's ratio ν_{ij} may be re-written in terms of derivatives of the cell parameters as follows:

$$\nu_{12} = (\nu_{21})^{-1} = -\frac{\mathrm{d}\varepsilon_2}{\mathrm{d}\varepsilon_1} = -\left(\frac{\mathrm{d}X_2}{X_2}\right)\left(\frac{\mathrm{d}X_1}{X_1}\right)^{-1}$$
$$= -\left(\frac{\mathrm{d}X_2}{\mathrm{d}\beta}\right)\left(\frac{\mathrm{d}X_1}{\mathrm{d}\alpha}\frac{\mathrm{d}\alpha}{\mathrm{d}\beta}\right)^{-1}\frac{X_1}{X_2}, \tag{6}$$

where $\mathrm{d}\varepsilon_i$ represents infinitesimally small strains in the Ox_i directions ($i, j = 1,2$) which may be defined in terms of infinitesimally small changes '$\mathrm{d}X_i$' in the value of 'X_i'.

Thus, by differentiating the expressions in (2) and (5) with respect to β and (1) with respect to α and substituting these, and the expressions in (1) and (2) into Eq. (6) we obtain:

$$\nu_{12} = (\nu_{21})^{-1} = -\frac{X_1\cos(\beta - \chi_R)}{2\sin(\alpha + \chi_R)[B + R\sin(\beta - \chi_R)]}. \tag{7}$$

Plots of the variation of the on-axis Poisson's ratio with the different geometric parameters, starting from different geometric setups are shown in Fig 6.

3 Discussion The derivations and graphs (Fig. 6) presented above clearly suggest that the system discussed here exhibits on-axis auxetic behaviour under certain conditions where the extent of auxeticity is dependent on the relative lengths of the ligaments, the size and aspect ratio of the node, and the angles between the ligaments and nodes.

Before we attempt to analyse in detail the properties afforded by this system, it is important to note that the parameters A, B, a, b, α and β must lie within certain ranges for the system to be physically constructible (i.e. we have constraints on the values the different geometric parameters can assume arising from geometric considerations). For example, if we want the system to be able to assume particular values of α, then we must put limits on the ligament of length A: for a given α within the range $0 \le \alpha \le \pi/2$, the minimum value that A can assume is $2a\cos(\alpha)$ as otherwise the nodes would overlap each other.

However rather than setting a minimum value on A, it is possible and more appropriate to discuss such constraints by limiting the values that the angles α and β can assume. In particular, for a given set of parameters (a, b, A, B), we shall let the range of values of the angles α and β to be $\alpha_{\min} \le \alpha \le \alpha_{\max}$ and $\beta_{\min} \le \beta \le \beta_{\max}$ respectively.

Firstly we note that the upper and lower bounds of α and β are determined by the requirement that the ligaments cannot cross into the nodes, which limits the values of α and β to lie within the maximum range of $\alpha, \beta \in [0, 3\pi/2]$. In this respect we note that since the angles α and β are dependent on each other through Eq. (5), the values of α are further restricted by the values that β can assume as illustrated in Fig. 7a, b which correspond to the situations were $\beta = 0$ and $\beta = 3\pi/2$ respectively. In fact, since for rectangular unit cells α and β are related to each other, the cell parameters (B, a, b, α, β) are not independent of each other but are related through Eq. (5) that can be written in the form:

$$B\sin(\alpha - \beta) = R\cos(\alpha - \chi_R).$$

Thus, once four out of the five geometric parameters (B, a, b, α, β) are set, the remaining one must have a specific value in order for the structure to be constructible. Assuming that we have fixed the lengths of the sides of the nodes and of the ligaments and letting β be within the range $0 \le \beta \le 3\pi/2$, we note that the corresponding maximum and minimum values of α are

$$\tan^{-1}\left[\frac{R\cos(\chi_R)}{B - R\sin(\chi_R)}\right] \le \alpha \le \tan^{-1}\left[\frac{B - R\cos(\chi_R)}{R\sin(\chi_R)}\right],$$

where the minimum occurs within the range of $\alpha \in [0, \pi]$ and the maximum is within the range $\alpha \in [\pi/2, 3\pi/2]$. These limits on α can be further simplified to

$$\underbrace{\tan^{-1}\left[\frac{a}{B - b}\right]}_{\text{between } 0-\pi} \le \alpha \le \underbrace{\tan^{-1}\left[\frac{B - a}{b}\right]}_{\text{between } \pi/2-3\pi/2}$$

by noting that $\chi_R = \tan^{-1}(b/a)$ and $R = \sqrt{a^2 + b^2}$.

In addition to this, for short ligaments A (i.e. $A < 2a$ or $A < 2b$) we must also avoid situations where the nodes overlap with each other as illustrated in Fig. 7c, d.

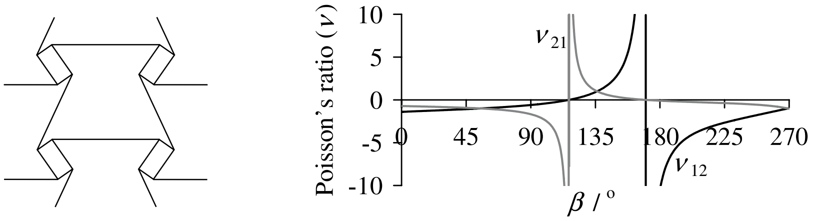

(a) The structure has $A = 9$, $B = 7$ $a = 3$ and $b = 1.5$.

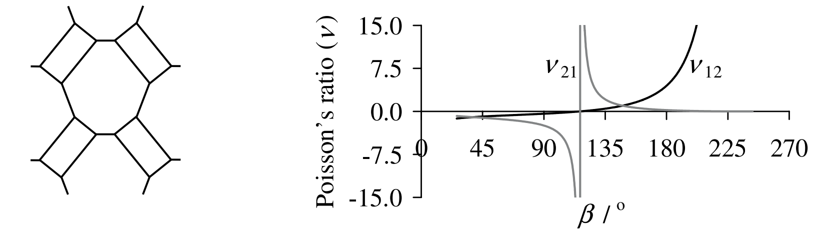

(b) The structure has $A = 1$, $B = 2$ $a = 3$ and $b = 1.5$.

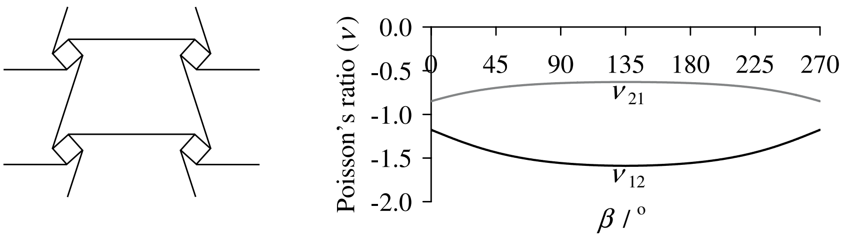

(c) The structure has $A = 9$, $B = 7$ and $a = b = 1.5$.

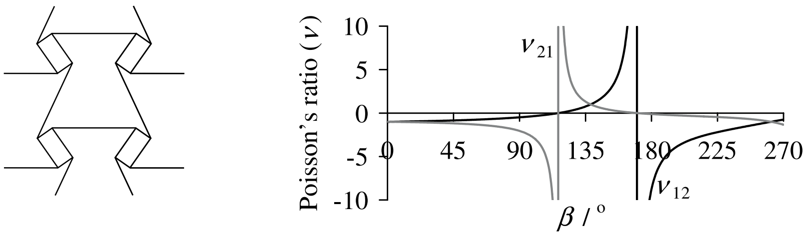

(d) The structure has $A = B = 7$, $a = 3$ and $b = 1.5$.

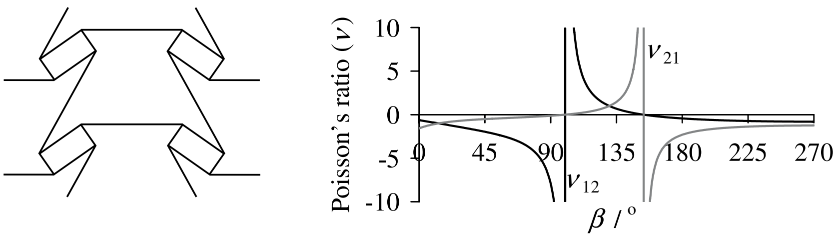

(e) The structure has $A = 6$, $B = 7$ $a = 1.5$ and $b = 3$.

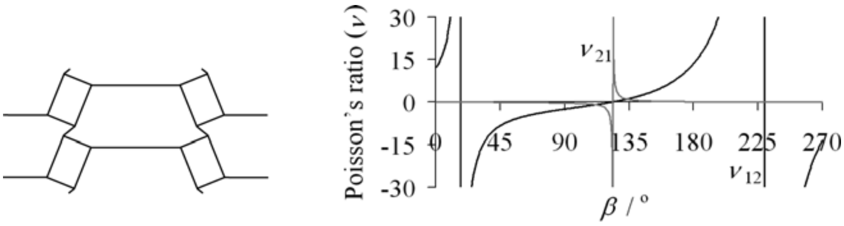

(f) The structure has $A = 6$, $B = 1$ $a = 3$ and $b = 2$.

Figure 6 Plots of the variation of the on-axis Poisson's ratio with β for various unit cell geometric parameters.

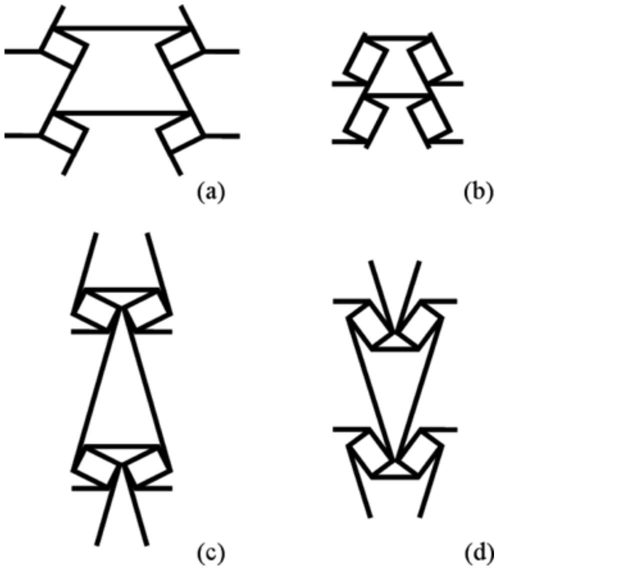

Figure 7 Conformations where the structure cannot be compressed or stretched any further due to some physical constraint.

Thus, the angle α is restricted to assume values where:

– the minimum limit that α can assume to ensure that the nodes do not overlap is within the range $[0, \pi/2]$ and in the case that $2a < A$, the lower bound will be given by the solution of the equation $2a\cos(\alpha) = A$, i.e. $\alpha = \cos^{-1}(A/(2a))$;

– the maximum value that α can assume to ensure that the nodes do not overlap is within the range of $[\pi, 3\pi/2]$ and in the case that $2b < A$, then the upper limit will be the solution of the equation $A = -2b\sin(\alpha)$ i.e. $\alpha = \sin^{-1}(-2b/A)$.

In view of all this, having fixed (a, b, A, B), the range of possible values for α are:

$$\alpha_{\min} \le \alpha \le \alpha_{\max}$$

where:

$$\alpha_{\min} = \begin{cases} \tan^{-1}\left[\dfrac{a}{B-b}\right] & A > 2a \\ \max\left\{\tan^{-1}\left[\dfrac{a}{B-b}\right], \cos^{-1}\left(\dfrac{A}{2a}\right)\right\} & A < 2a \end{cases}$$

where $\alpha_{\min} \in [0, \pi]$,

$$\alpha_{\max} = \begin{cases} \tan^{-1}\left[\dfrac{B-a}{b}\right] & A > 2b \\ \max\left\{\tan^{-1}\left[\dfrac{a}{B-b}\right], \sin^{-1}\left(\dfrac{-2b}{A}\right)\right\} & A < 2b \end{cases}$$

where $\alpha_{\min} \in \left[\dfrac{\pi}{2}, \dfrac{3\pi}{2}\right]$,

from which we may determine the corresponding lower and upper bounds for β.

Having established the upper and lower boundaries of the geometric parameters that make up the meta-tetrachirals, we now examine the possible values that the on-axis Poisson's ratios of these systems can assume.

First of all we note that the model presented by Eq. (7) can be used to represent the system in Fig. 3b (i.e. when the ligaments are tangential to a circular node, a system which may be considered as the 'equivalent' of Lakes' hexachiral model [42]) if both ligaments in the hinging model make an angle of 90° to the diagonals of the rectangular nodes. This requires that $(\pi/2) - \chi_R + \beta = \pi/2 \Rightarrow \beta = \chi_R$ and $\chi_R + \alpha = \pi/2$. On substituting these values in Eq. (7), the Poisson's ratio for this particular case, the hinging model reduces to:

$$\nu_{12} = (\nu_{21})^{-1} = -\frac{A}{B} . \qquad (8)$$

In the particular case when all the ligaments in the system have the same length (i.e. $A = B$), then the Poisson's ratio would assume a value of –1, as was the case with Lakes's hexachiral model [42]. In other words, when the ligaments are tangentially attached to the nodes, the on-axis Poisson's ratio will always be negative and equal to the negative of the ratio of length of the ligaments. In fact, since $A > 0$ and $B > 0$, the on-axis Poisson's ratio will range between 0 and $-\infty$. However, for the more general cases, the on-axis Poisson's ratios of the hinging model is more complex and can assume either negative or positive values, as illustrated in Fig. 6.

Considering the Poisson's ratio in terms of the partial derivates,

$$\nu_{12} = -\frac{d\varepsilon_2}{d\varepsilon_1} = -\frac{dX_2}{d\beta}\left(\frac{dX_1}{d\alpha}\right)^{-1}\left(\frac{d\alpha}{d\beta}\right)^{-1}\frac{X_i}{X_j} , \quad i, j = 1, 2 ,$$

for on-axis negative Poisson's ratios, we require:

$$\frac{dX_2}{d\beta}\left(\frac{dX_1}{d\alpha}\right)^{-1}\left(\frac{d\alpha}{d\beta}\right)^{-1}\frac{X_i}{X_j} > 0 . \qquad (9)$$

Since the unit cell lengths are always positive (i.e. both $X_1, X_2 > 0$) for all the possible values of β, this requirement reduces to the constraint that:

(i) the three derivates $\dfrac{dX_2}{d\beta}, \dfrac{dX_1}{d\alpha}, \dfrac{d\alpha}{d\beta} > 0$, or

(ii) two of the derivatives $\dfrac{dX_2}{d\beta}, \dfrac{dX_1}{d\alpha}, \dfrac{d\alpha}{d\beta}$ are negative,

while the other one is positive, giving three possible combinations.

The above considerations give rise to the following four cases:

Case 1, referring to the situation when $\dfrac{dX_2}{d\beta}, \dfrac{dX_1}{d\alpha}, \dfrac{d\alpha}{d\beta} > 0$:

$$\cos(\beta - \chi_R) > 0 , \qquad \sin(\alpha + \chi_R) > 0 ,$$

$$B + R\sin(\beta - \chi_R) > 0 .$$

Case 2, referring to the situation when $\frac{dX_2}{d\beta}, \frac{dX_1}{d\alpha} < 0$ and $\frac{d\alpha}{d\beta} > 0$:

$$\cos(\beta - \chi_R) < 0 , \qquad \sin(\alpha + \chi_R) < 0 ,$$

$$B + R\sin(\beta - \chi_R) > 0 .$$

Case 3, referring to the situation when $\frac{dX_2}{d\beta}, \frac{d\alpha}{d\beta} < 0$ and $\frac{dX_1}{d\alpha} > 0$:

$$\cos(\beta - \chi_R) < 0 , \qquad \sin(\alpha + \chi_R) > 0 ,$$

$$B + R\sin(\beta - \chi_R) < 0 .$$

Case 4, referring to the situation when $\frac{dX_2}{d\beta} > 0$ and $\frac{dX_1}{d\alpha}, \frac{d\alpha}{d\beta} < 0$:

$$\cos(\beta - \chi_R) > 0 , \qquad \sin(\alpha + \chi_R) < 0 ,$$

$$B + R\sin(\beta - \chi_R) < 0 .$$

To discuss the particulates of these cases, it is convenient to consider separately the situations where (i) $B > R$ and (ii) $B < R$.

3.1 The properties of systems where *B* > *R* We first consider the situation when $B > R$ where it follows that $d\alpha/d\beta > 0$ since $B + R\sin(\beta - \chi_R) > 0$ (the sine of an angle is always between –1 and +1). Thus, cases 3 and 4 cannot occur, while the third condition in cases 1 and 2 is automatically satisfied. This reduces these cases to:

$$\text{Case 1:} \quad \cos(\beta - \chi_R) > 0 \quad \text{and} \quad \sin(\alpha + \chi_R) > 0$$

$$\Rightarrow \beta < \frac{\pi}{2} + \chi_R \quad \text{and} \quad \alpha < \pi - \chi_R ,$$

$$\text{Case 2:} \quad \cos(\beta - \chi_R) < 0 \quad \text{and} \quad \sin(\alpha + \chi_R) < 0$$

$$\Rightarrow \beta > \frac{\pi}{2} + \chi_R \quad \text{and} \quad \alpha > \pi - \chi_R ,$$

i.e., using the relation between α and β (Eq. (5)) we obtain:

$$\text{Case 1:} \quad \alpha < \frac{\pi}{2} + \chi_R \quad \text{and} \quad \alpha < \pi - \chi_R ,$$

$$\text{Case 2:} \quad \alpha > \frac{\pi}{2} + \chi_R \quad \text{and} \quad \alpha > \pi - \chi_R .$$

Thus, the range of values can be divided into three regions depending on the value of α and we find that:

– In the range $\alpha_{\min} < \alpha < \min[\pi - \chi_R, (\pi/2) + \chi_R]$ the Poisson's ratios are negative.

– In the range $\min[\pi - \chi_R, (\pi/2) + \chi_R] < \alpha < \max \times [\pi - \chi_R, (\pi/2) + \chi_R]$ the Poisson's ratios are positive.

– In the range $\max[\pi - \chi_R, (\pi/2) + \chi_R] < \alpha < \alpha_{\max}$ the Poisson's ratios are negative.

This suggests that the Poisson's ratio changes sign at most twice within the region $\alpha_{\min}$ to $\alpha_{\max}$, i.e. when $\alpha = \pi - \chi_R$ and when $\alpha = (\pi/2) + \chi_R$.

As illustrated in Fig. 8a, the condition when $\alpha = \pi - \chi_R$ corresponds to the situation when the ligaments of length A are aligned with the diagonal across the node that joins them and with the Ox_1 direction. This means that a force applied along the Ox_1 direction would not produce a deformation, which implies that the structure is locked along the Ox_1 direction (i.e. a situation when the Young's modulus in the Ox_1 direction would have an infinite value if the structure deforms solely through hinging). From a mathematical point of view, we note that this change in the sign of the Poisson's ratios arises from having the partial derivative $dX_1/d\alpha = 0$. This partial derivative is found in the denominator of the equation for ν_{12} and in the numerator of the equation for ν_{21} (see Eq. (7)), thus suggesting that the Poisson's ratio ν_{12} will change sign asymptotically when $\alpha = \pi - \chi_R$ (tending to $-\infty$ from one side and to $+\infty$ from the other) whilst the Poisson's ratio ν_{21} changes sign in a continuous manner (i.e. $\nu_{21} = 0$ when $\alpha = \pi - \chi_R$). Note that the asymptotic behaviour of the Poisson's ratio ν_{12} as $\alpha \to \pi - \chi_R$ is characteristic of 'locked' systems (see discussion relating to the idealised Type I rotating rectangles model [48]). Such features are clearly illustrated in Fig. 6a, b, d, e.

Similarly, as illustrated in Fig. 8b, the condition when $\alpha = (\pi/2) + \chi_R$ corresponds to the circumstance when the ligaments of length B are aligned with the diagonal across the node that joins them and with the Ox_2 direction. This means that a force applied along the Ox_2 direction would not produce a moment around the node. In practice, this implies that the structure is locked along this direction (i.e. a situation when the Young's modulus in the Ox_2 direction would have an infinite value if the structure deforms solely through hinging). From a mathematical point of view, once again we note that this change in the sign of the Poisson's ratios arises from having a partial derivative being equal to

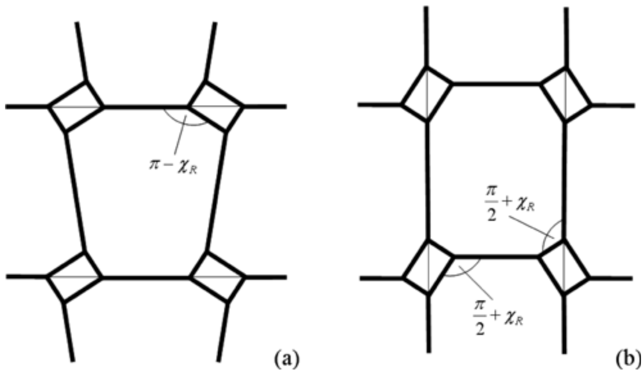

Figure 8 Condition corresponding to the situation when (a) the ligaments of length A and (b) the ligaments of length B are aligned with the diagonal across the node that joins them.

zero, in this case $\mathrm{d}X_2/\mathrm{d}\beta = 0$. This partial derivative is found in the numerator of the equation for ν_{12} and in the denominator of the equation for ν_{21} (see Eq. (7)), thus suggesting that the Poisson's ratio ν_{12} changes sign in a continuous manner (i.e. $\nu_{12} = 0$ when $\alpha = (\pi/2) + \chi_R$) whilst the Poisson's ratio ν_{21} will change sign asymptotically when $\alpha = (\pi/2) + \chi_R$ (tending to $+\infty$ from one side and to $-\infty$ from the other, a situation which once again corresponds to having a 'locked' system). Such features are clearly illustrated in Fig. 6a, b, d, e.

We also note that in the special case when the nodes are square, i.e. when $a = b$, we find that $\chi_R = \pi/4$ and so $\alpha = \pi - \chi_R = (\pi/2) + \chi_R = 3\pi/4$. In such a case, the positive region of the on-axis Poisson's ratios is not observed, as clearly illustrated in Fig. 6c. Furthermore we note that both $\mathrm{d}X_1/\mathrm{d}\alpha$ and $\mathrm{d}X_2/\mathrm{d}\beta$ would be simultaneously equal to zero when $\alpha = 3\pi/4$ leading to the situation of having a zero divided by a zero in Eq. (7) (i.e. the Poisson's ratio is undefined), which corresponds to the situation where the structure is simultaneously locked in both the Ox_1 and Ox_2 directions. A similar situation was encountered in the rotating squares model [49, 50] when the angle between the squares was 90°.

3.2 The properties of systems where *B* < *R* If we now allow for the possibility that $B < R$, the situation is much more complex as it might be possible to satisfy the condition for $B + R\sin(\beta - \chi_R) < 0$ in one or both of the following regions:

$$0 < \beta < \chi_R - \omega \quad \text{or} \quad \pi + \omega - \chi_R < \beta < 3\pi/2 \ ,$$

where $\omega = \sin^{-1}(B/R)$.

This means that all four Cases 1–4 mentioned above need to be considered in order to determine the sign of the Poisson's ratio.

In terms of α these regions can be expressed as

$$\alpha_{\min} < \alpha < (\pi/2) - \omega \quad \text{or} \quad \chi_R - \psi < \alpha < \alpha_{\max} \ ,$$

where ψ is defined as

$$\psi = \tan^{-1}\left[\frac{R + B\sin(2\chi_R - \omega)}{B\cos(2\chi_R - \omega)}\right].$$

Combining these conditions with those obtained previously, we conclude that the value of the Poisson's ratio in the allowed range of α depends on the attainability and magnitude of the angles $\{(\pi/2) - \omega, \chi_R - \psi, \pi - \chi_R, (\pi/2) + \chi_R\}$. As α increases the Poisson's ratio will change sign each time α exceeds one of these angles. So in the allowed region of α, the Poisson's ratio will alternate between negative and positive values as exemplified in Fig. 6f.

The reasons for the change of sign in the Poisson's ratio when $\alpha = \pi - \chi_R$ and $(\pi/2) + \chi_R$ are the same as those for the situation when $B > R$. The increase in the number of values of α that make the Poisson's ratio change sign when $B < R$ is linked to a change of sign of $\mathrm{d}\alpha/\mathrm{d}\beta$. As can be seen from Fig. 9 if $B < R$ at the beginning and/or at the end of the allowed regions of α, an increase in β would bring about a decrease in the value of α, and a decrease in β would bring about an increase in the value of α.

The attainability and location of the point or points at which $\mathrm{d}\alpha/\mathrm{d}\beta = 0$ are also of interest. This condition is satisfied when the ligaments of length B are aligned in the same direction as the ligaments of length A. This can be achieved in one of the two situations shown in Fig. 10, with the one illustrated in Fig. 10a being possible if $B \le b$ while the one depicted in Fig. 10b being attainable if $B \le a$. In these situations, considering the moments around the node, it can be deduced that the ligaments of length A will create a moment that has an equal but opposite direction to that created by the ligaments of length B. Thus the structure will be effectively locked along the Ox_1 direction. This is confirmed by the fact that $\mathrm{d}\alpha/\mathrm{d}\beta$ is in the denominator of ν_{12} and as a result the Poisson's ratio will tend to infinity when $\mathrm{d}\alpha/\mathrm{d}\beta \to 0$ as was the case of $\mathrm{d}X_1/\mathrm{d}\alpha$.

4 Conclusions In this work we have shown that Lakes's and Sigmund's auxetic structures constructed from chiral building blocks exhibiting rotational symmetry of order n are two examples of a larger set of structures that can be constructed from such chiral building blocks. Furthermore, we showed that when the rotational symmetry of the chiral building block is relaxed, a new class of structures, collectively referred to as 'meta-chirals' can be obtained which can be seen as an intermediate between the 'chirals' and 'anti-chirals'. We have analysed one example of this novel 'meta-chirals' class of structures: the tetra-

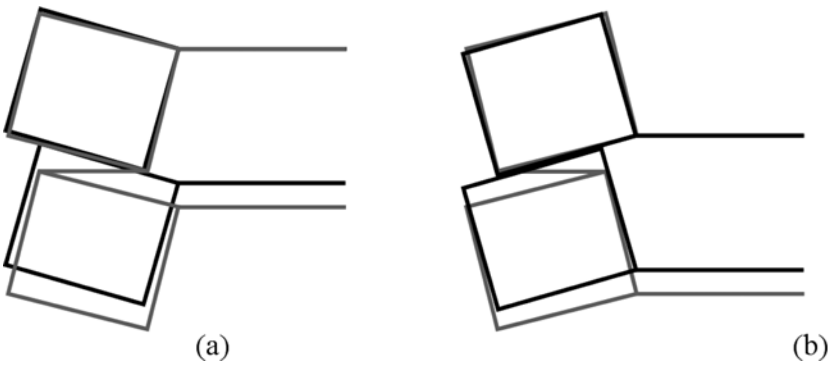

Figure 9 A figure showing that an increase in β brings about a decrease in α when $B < R$, for the (a) fully closed system and (b) fully open system.

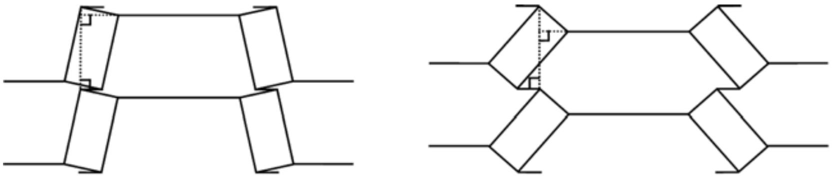

(a) (b)

Figure 10 Situation when the ligaments of lenght *A* and *B* are aligned in the same direction.

meta-chiral system. This is a structure where four ligaments are attached to a central node where the rotational symmetry is less than four. Analytical modelling of the tetrameta-chiral systems deforming through hinging were produced and these suggested that when the meta-tetrachirals are constructed from rectangular nodes and deform though hinging (i.e. through changes in the angles between the nodes and the ligaments), these systems may exhibit either auxetic or conventional behaviour where the Poisson's ratios can range from $-\infty$ to $+\infty$. The actual values of the Poisson's ratio where shown to be dependant on the geometric parameters of the systems. This behaviour in the Poisson's ratios where, for example, the Poisson's ratio can be more negative than -1 is possible as a result of the fact that the system is highly anisotropic. (The model presented here only discusses the Poisson's ratios for loading in preferred directions (on-axis), coinciding with the symmetry axes of the system.)

These meta-tetrachiral systems can be considered to be the first example of this new subclass of 'chirals' that are capable of exhibiting auxetic behaviour, hence introducing the concept that many more systems made from chiral building blocks may be constructed if we relax the condition that the rotational symmetry is equal to the number of ligaments attached to the nodes. Thus we have confirmed the potential of the chiral unit proposed by Lakes [42] and Sigmund [43] for generating auxetic behaviour.

The equations derived here are expected to be useful to experimentalists who may wish to construct novel auxetic systems based on the meta-tetrachiral proposed here. Through these equations, they may be able to produce systems which exhibit particular values of the Poisson's ratios thus producing systems which are tailor-made for particular practical applications. In this respect, it is also important to note that the equations derived here suggest that the Poisson's ratio of this system is once again scale independent and thus the meta-chirals proposed here may be constructed at any scale ranging from the nanolevel to the macroscale.

Acknowledgements The help of Victor Zammit and Daphne Attard from the Faculty of Science, University of Malta is gratefully acknowledged. Part of this research was financed through the FP6 project CHISMACOMB.

References

[1] K. E. Evans, M. A. Nkansah, I. J. Hutchinson, and S. C. Rogers, Nature **353**, 124 (1991).
K. W. Wojciechowski, A. Alderson, K. L. Alderson, B. Maruszewski, and F. Scarpa, phys. stat. sol. (b) **244**, 813 (2007).
[2] R. S. Lakes, http://silver.neep.wisc.edu/~lakes/SelArticl.htm
[3] J. N. Grima and K. E. Evans, Chem. Commun. **16**, 1531 (2000).
[4] S. P. Timoschenko and J. N. Goodier, Theory of Elasticity (McGraw Hill, New York, 1970).
[5] B. M. Lempriere, AIAA J. **6**, 2226 (1968).
[6] K. W. Wojciechowski, J. Phys. Soc. Jpn. **72**, 1819 (2003).
[7] L. J. Gibson, M. F. Ashby, G. S. Schajer, and C. I. Robertson, Proc. R. Soc. Lond. A **382**, 25 (1982).
[8] R. F. Almgren, J. Elast. **15**, 427 (1985).
[9] D. Prall and R. S. Lakes, Int. J. Mech. Sci. **39**, 305 (1997).
[10] A. Spadoni, M. Ruzzene, and F. Scarpa, phys. stat. sol. (b) **242**, 695 (2005).
[11] K. W. Wojciechowski, Mol. Phys. **61**, 1247 (1987).
[12] K. W. Wojciechowski and A. C. Branka, Phys. Rev. A **40**, 7222 (1989).
[13] K. W. Wojciechowski, J. Phys. A, Math. Gen. **36**, 11765 (2003).
[14] R. S. Lakes, Science **235**, 1038 (1987).
[15] K. E. Evans, M. A. Nkansah, and I. J. Hutchinson, Acta Metall. Mater. **2**, 1289 (1994).
[16] J. B. Choi and R. S. Lakes, J. Compos. Mater. **29**, 113 (1995).
[17] N. Chan and K. E. Evans, J. Cellular Plast. **34**, 231 (1998).
[18] C. W. Smith, J. N. Grima, and K. E. Evans, Acta Mater. **48**, 4349 (2000).
[19] J. N. Grima, A. Alderson, and K. E. Evans, J. Phys. Soc. Jpn. **74**, 1341 (2005).
[20] K. E. Evans and B. D. Caddock, J. Phys. D, Appl. Phys. **22**, 1883 (1989).
[21] A. Alderson and K. E. Evans, J. Mater. Sci. **30**, 3319 (1995).
[22] A. Alderson and K. E. Evans, J. Mater. Sci. **32**, 2797 (1997).
[23] R. H. Baughman and D. S. Galvao, Nature **365**, 635 (1993).
[24] C. B. He, P. W. Liu, and A. C. Griffin, Macromolecules **31**, 3145 (1998).
[25] J. N. Grima, J. J. Williams, and K. E. Evans, Chem. Commun. **32**, 4065 (2005).
[26] G. Y. Wei, phys. stat. sol. (b) **242**, 742 (2005).
[27] R. H. Baughman, J. M. Shacklette, A. A. Zakhidov, and S. Stafstrom, Nature **392**, 362 (1998).
[28] A. Yeganeh-Haeri, D. J. Weidner, and D. J. Parise, Science **257**, 650 (1992).
[29] N. R. Keskar and J. R. Chelikowsky, Phys. Rev. B **46**, 1 (1992).
[30] H. Kimizuka, H. Kaburaki, and Y. Kogure, Phys. Rev. Lett. **84**, 5548 (2000).
[31] A. Alderson and K. E. Evans, Phys. Rev. Lett. **89**, 225503 (2002).
[32] H. Kimizuka, H. Kaburaki, and Y. Kogure, Phys. Rev. B **67**, 024105 (2003).
[33] A. Alderson, K. L. Alderson, K. E. Evans, J. N. Grima, and M. Williams, J. Met. Nano. Mater. **23**, 55 (2004).

[34] A. Alderson, K. L. Alderson, K. E. Evans, J. N. Grima, M. Williams, and P. J. Davies, phys. stat. sol. (b) **242**, 499 (2005).
[35] J. N. Grima, R. Gatt, A. Alderson, and K. E. Evans, J. Mater. Chem. **15**, 4003 (2005).
[36] J. N. Grima, R. Gatt, A. Alderson, and K. E. Evans, Mater. Sci. Eng. A **423**, 214 (2006).
[37] J. N. Grima, R. Jackson, A. Alderson, and K. E. Evans, Adv. Mater. **12**, 1912 (2000).
[38] J. N. Grima, Ph.D. thesis, University of Exeter, Exeter, UK (2000).
[39] R. S. Lakes and K. Elms, J. Compos. Mater. **27**, 1193 (1993).
[40] A. Alderson, Chem. Ind. **10**, 384 (1999).
[41] F. Scarpa, J. Giacomin, Y. Zhang, and P. Pastorino, Cellular Polym. **24**, 253 (2005).
[42] R. S. Lakes, J. Mater. Sci. **26**, 2287 (1991).
[43] O. Sigmund, S. Torquato, and I. A. Askay, J. Mater. Res. **13**, 1038 (1998).
[44] K. E. Evans, A. Alderson, and F. R. Attenborough, J. Chem. Soc. Faraday Trans. **91**, 2671 (1995).
[45] I. G. Masters and K. E. Evans, Compos. Struct. **34**, 1 (1996).
[46] J. N. Grima and K. E. Evans, J. Mater. Sci. **41**, 3193 (2006).
[47] J. N. Grima, R. Gatt, P. S. Farrugia, A. Alderson, and K. E. Evans, ASME International Mechanical Engineering Congress Proceedings (2005).
[48] J. N. Grima, A. Alderson, and K. E. Evans, phys. stat. sol. (b) **242**, 561 (2005).
[49] J. N. Grima and K. E. Evans, J. Mater. Sci. Lett. **19**, 1563 (2000).
[50] Y. Ishibashi and M. J. Iwata, J. Phys. Soc. Jpn. **69**, 2702 (2000).